International Journal of ChemTech Research
CODEN(USA): IJCRGG ISSN : 0974-4290
Vol.5, No.4, pp 2018-2026, April-June 2013

Synthesis and Characterization of L-Methioninium Nitrate Single Crystal for Nonlinear Optical Applications

P. Vasudevan[1,2], S. Sankar[1,*] and D. Jayaraman[3]

[1] Department of Physics, MIT Campus, Anna University, Chennai 600 044, India.
[2] Department of Physics, SKR Engineering College, Chennai 600 123, India.
[3] Department of Physics, Presidency College, Chennai 600 005, India.

***Corres. Author: ssankarmit@gmail.com**
Tel: +9144-22516136, Fax: +9144-22516136

Abstract: Nonlinear optical crystal of L-methioninium nitrate was grown by slow evaporation method from aqueous solution at room temperature. The lattice parameters and crystal structure of the grown crystal were identified and confirmed using single crystal X-ray diffraction analysis. Fourier transform infrared spectroscopy analysis was made to study the vibrational functional groups present in the crystal. Molecular structure of the grown crystal was discussed using ^{1}H NMR and ^{13}C NMR studies. Optical absorption range of the grown crystal was measured by UV-VIS-NIR spectrophotometer. Thermal stability and decomposition of the grown crystal were studied using thermogravimetric and differential thermal analysis. Mechanical strength of the grown crystal was analyzed using Vickers microhardness tester. Nonlinear optical property of the crystal was confirmed by Kurtz and Perry powder technique.
Keywords: Crystal growth, Nuclear magnetic resonance (NMR), Optical absorption,Thermal properties, Mechanical properties, Nonlinear optical material.

1. Introduction

The search for amino acid derivatives of nonlinear optical (NLO) materials has stimulated considerable interest over the past two decades for their potential applications in optical communications, laser technology, optical storage devices and optoelectronics [1-3]. Especially organic materials are the leading practical materials for fabricating optoelectronic devices. In this respect, organic amino acids are intriguing materials for NLO applications because they contain proton donor carboxyl acid groups (COOH) and proton acceptor amino groups (NH_2) [4]. The importance of amino acids in NLO applications is due to the fact that all the amino acids have molecular chirality, absence of strongly conjugated bonds and zwitterionic nature of the molecule and more importantly they crystallize in non-centrosymmetric space group [5,6]. Therefore, attention has been focused on amino acid complexes and they seemed to possess all characteristics features for photonics and NLO applications. Hence, we have chosen L-methionine, one among the two sulphur containing proteinogenic amino acids, the other one being cysteine for forming amino acid complexes. L-methionine has been exploited for the formation of salts with different organic and inorganic acids using solution growth technique. Recently, several salts of L-methionine such as bis(L-methioninium) sulfate, L-methionine L-methioninium perchlorate, etc., were reported [7-12]. Considerable efforts have been made to combine amino acids with nitric acid to produce a promising nonlinear optical material [13-15]. In this direction, Pandiyarajan et al have reported only the crystal structure and vibrational spectral studies of L-methioninium nitrate [LMN] [16,17]. Literature survey reveals that other detailed characterization studies of LMN have not been reported so far. Hence, in the present

investigation, we report the synthesis and characterization of the title compound for NLO applications. The SHG behaviour was observed in the material and reported for the first time. The grown crystal was characterized using the studies of single crystal XRD, FTIR, NMR, UV-VIS-NIR spectral analysis, thermal behaviour, microhardness and NLO test.

2. Experimental

2.1 Synthesis and purification

Analytical grade of L-methionine and nitric acid were taken as the starting materials for synthesizing LMN. A solution was prepared by dissolving L-methionine and nitric acid in water with 1:1 molar ratio and stirred using magnetic stirrer to get homogeneous solution. The solution was then allowed for slow evaporation at room temperature. As a result, the solution gradually reached supersaturation leading to nucleation phenomenon followed by the growth mechanism. Well transparent and colourless crystals of LMN with dimensions of 10 × 5 × 3 mm^3 were formed after a period of 20 days. The product was then purified by recrystallization process. The as-grown LMN crystal is shown in Figure 1. The reaction for the synthesized crystal is given as follows:

$$C_5H_{11}NO_2S + HNO_3 \rightarrow C_5H_{12}NO_2S^+ . NO_3^- \quad (1)$$

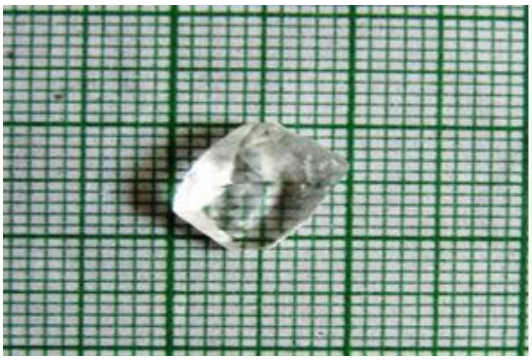

Fig. 1 -As-grown LMN crystal

2.2 Characterization

Single crystal XRD studies were carried out using Bruker Kappa APE XII single X-ray diffractometer to determine the lattice parameters and the space group of the grown LMN crystal. The FTIR spectrum was recorded in the range of 500 - 4000 cm^{-1} using IR Prestige-21 (Shimadzu) with KBr pellet technique to understand the functional groups present in the grown crystal. The ^1H NMR and ^{13}C NMR spectral experiments were performed for the crystal and the spectral data were recorded in a magnetic field of 11.75 tesla (500 MHz) using Bruker AV III Fourier Transformed NMR spectrometer (For ^1H NMR data ν_0 = 500 MHz and ^{13}C NMR data ν_0 =125 MHz) for analyzing molecular structure. Optical absorption measurements were made using Perkin Elmer Lamda 35 UV-VIS-NIR spectrophotometer with a resolution of 2 nm in the region from 200 nm to 1200 nm to measure the absorption range of the crystal. The TGA and DTA of the sample were studied using the instrument NETZSCH STA 449 F1and F3 Jupiter series in the temperature range of 30º C to 500º C under nitrogen atmosphere to understand the thermal behaviour. Microhardness of the grown crystal was analyzed using REICHERT MD 4000E ULTRA microharness tester with diamond pyramid indenter attached to an optical microscope. Nonlinear optical property of LMN crystals was confirmed by the Kurtz and Perry powder technique using Q-switched high energy Nd:YAG laser (QUANTA RAY model LAB-170-10).

3. Results and discussion

3.1 Single crystal XRD analysis

A selected transparent grown crystal was subjected to single crystal X-ray diffractometer to determine crystal structure and lattice parameters. Single crystal XRD analysis reveals that the grown crystal belongs to monoclinic structure with non-centrosymmetirc space group $P2_1$.The lattice parameters were found to be a = 10.68 (2) Å, b = 5.47 (2) Å, c = 16.72 (6) Å; α = γ = 90º, β = 100.7º with unit cell volume V = 983.3 $Å^3$. These

lattice parameters values are found to be in good agreement with the reported values [16]. The non-centrosymmetric nature of the grown crystal fulfills the important criterion for an NLO crystal.

3.2 FTIR Studies

In order to identify the functional groups present in LMN crystals, FTIR spectrum was recorded in the range between 4500 cm^{-1} and 500 cm^{-1} by the KBr pellet technique. The resulting spectrum is shown in Figure 2. The peak in the higher energy band region at 3427 cm^{-1} is assigned to NH asymmetric stretching and absorption peak at 1732 cm^{-1} is due to COO^- stretching. NH_3^+ asymmetric deformation and COO^- stretching are assigned to the peaks at 1619 cm^{-1} and 1190 cm^{-1} respectively. The peaks at 1138 cm^{-1} and 538 cm^{-1} are attributed to NH_3^+ rocking and NH_3^+ torsion respectively. The absorption band that appears around 652 cm^{-1} is due to the plane in deformation mode of the O – C = O group. These peak assignments confirm the presence of carbonyl group and amino group in LMN. The presence of NO_3^- is clearly revealed by the peaks at 1048 cm^{-1}, 825 cm^{-1} and 699 cm^{-1}. The peaks at 1034 cm^{-1} and 1072 cm^{-1} are assigned to C-N stretching vibrations and the band observed at 1100 cm^{-1} is due to C-C-N stretching vibrations. These peak assignments indicate the asymmetric motion of carbon branched against its neigbours. The presence of methyl and methylene groups has been identified by the peaks positioned at 2923 cm^{-1}, 1381 cm^{-1}, 1238 cm^{-1}, 983 cm^{-1}, 772 cm^{-1} and 756 cm^{-1}. The IR peak assignments are found to be in good agreement with the literature [17]. The FTIR spectrum obtained thus shows the presence of functional groups of LMN single crystal.

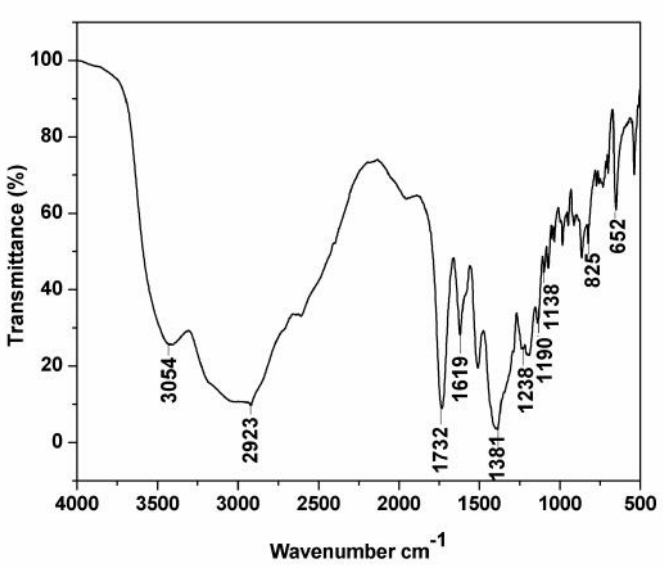

Fig. 2 FTIR spectrum of LMN crystal

3.3 NMR Studies

^1H NMR and ^{13}C NMR studies were analyzed to confirm the molecular structure of organic compounds. Figure 3 shows the ^1H NMR spectrum of LMN crystal. The doublet peaks due to δ = 2.030 ppm indicates the presence of $–CH_3$ group in LMN. The quadret peaks due to the signal at δ = 2.114 ppm are attributed to the $-CH_2$ group attached to sulphur atom and the adjacent quadret peaks at δ = 2.209 ppm corresponds to the neigbouring methylene group. The broad peak at δ = 4.144 ppm is attributed to NH_3^+. The triplet peaks corresponding to δ = 2.613 ppm are due to highly destined –CH proton. These signals clearly explain the molecular structure and the absence of impurities in the grown crystal.

^{13}C NMR spectrum of LMN material is shown in Figure 4. In the spectrum, four carbon atoms are identified with respect to four different peaks located at various chemical environments. The signal at δ = 171.766 ppm is attributed to the presence of carboxylic group in L-methionine. The signal at δ = 51.850 ppm is due to carbon atom connected to amino group in LMN. The resonance peaks at δ = 28.567 ppm and δ = 28.902 ppm indicate the presence of two CH (isopropyl) in LMN. Methyl group CH_3 in LMN is confirmed by the peak at δ = 13.850 ppm. As there are no other signals except the above in the spectrum, the purity of the compound is confirmed.

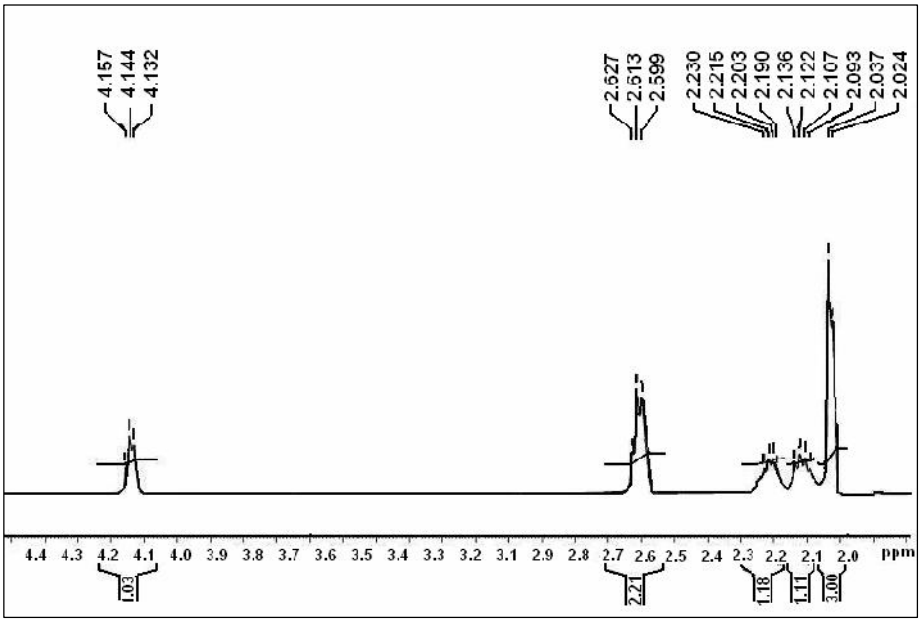

Fig. 3 ^{1}H NMR spectrum of LMN crystal

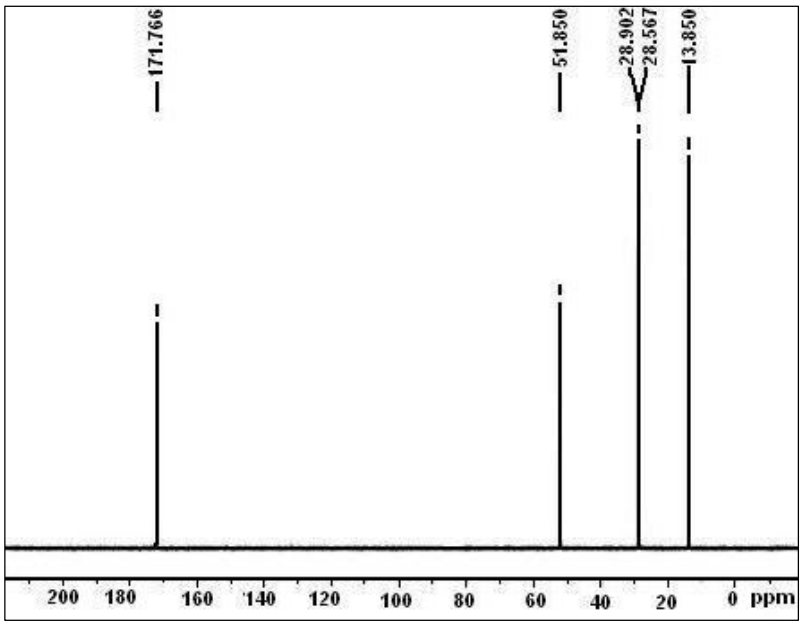

Fig. 4 ^{13}C NMR spectrum of LMN crystal

3.4 Optical Studies

UV-VIS-NIR absorption spectrophotometer was used to record the absorption spectrum in the range between 200 nm and 1200 nm. From the observed spectrum (Figure 5), the lower cut-off wavelength is found to be 325 nm and there is no absorption peak in the visible region and near the infrared region which indicates the absence of overtones [18]. The absorption peaks obtained in the range between 200 nm and 350 nm shows n to π* transitions of carbonyl group [19]. The absence of absorption in the near infrared region provides the access to the laser wavelength of 1064 nm from Nd: YAG source for second harmonic generation. Hence, UV

absorption studies reveal that the grown LMN crystal is one of the suitable materials for exhibiting second harmonic generation in the entire visible and near infrared region. The Tauc's plot of $(\alpha h\nu)^2$ against the photon energy ($h\nu$) at room temperature (Figure 6) shows a linear behaviour, (α-absorption coefficient and h-Planck's constant) which can be considered as an evidence of the indirect transition. Using Tauc's plot, the band gap of the LMN crystal was found to be 3.66 eV.

3.5 Thermal Studies

Thermogravimetry analysis (TGA) and differential thermal analysis (DTA) were made to investigate the thermal properties of the grown crystal. A ceramic crucible was used for heating the sample and the sample was heated in an atmosphere of nitrogen at a heating rate of 20ºC per minute for the temperature range between 30ºC and 500ºC to record the results. The recorded plots are shown in Figure 7. The TGA curve indicates that the LMN crystal is thermally stable up to 142ºC. On heating above this temperature, a weight loss of 68.81% occurs between 143º C and 248º C due to the release of CO, and H_2O. Further, 16.82% weight loss was observed between 249º C and 499º C due to release of NH_3, H_2 and CH_4 vapour molecules. Almost all the gas molecules were removed and finally the residual mass was obtained at 497.8˚ C. In the DTA curve, a sharp endothermic peak was observed at 142º C, indicating the melting point of LMN. It shows that there is no decomposition before the melting of the material. Hence, for NLO applications of the crystal the maximum temperature is limited to 142º C.

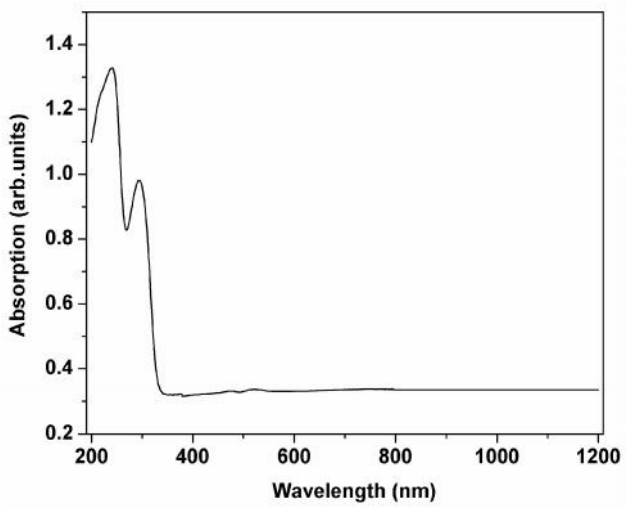

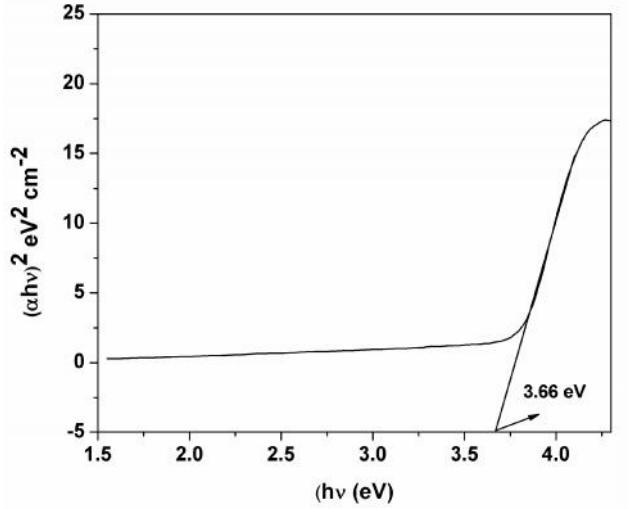

Fig. 5 UV-VIS-NIR absorption spectrum of LMN crystal **Fig. 6 Band gap of LMN crystal**

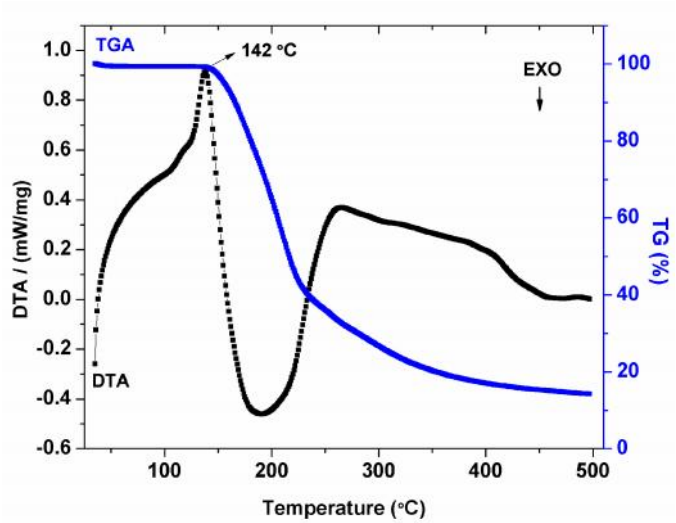

Fig. 7 TG-DTA curve of LMN crystal

3.6 Vickers microhardness

Analysis of mechanical property of the grown crystal is also important for the fabrication of electronic and optical devices. Microharness studies have been carried out on (001) face a selected well transparent single crystal using microharness tester, fitted with a Vickers diamond pyramidal indenter [20]. To get accurate results of hardness of the grown crystal indentations were made on the LMN crystals with applied load ranging from 5g to 35g. The time of indentation was kept constant for 10s. Five indentations were made on each surface under examination for the same load and the mean diagonal length was measured. To avoid surface defects, the distance between consecutive indentations was kept more than five times the diagonal length of the indentation mark. The diagonal length of indentation mark was measured using a micrometer eyepiece at a magnification of 80×. The value of Vickers microhardness was calculated using the relation,

$$H_v = 1.8544\ P/d^2\ \ kg/mm^2 \qquad (2)$$

where, P is the applied load and d is the mean diagonal length of the indenter impression. Figure 8 shows the variation of hardness with the applied load. It is observed that the hardness of LMN increases with increase of load up to 25g which indicates the reverse indentation size effect [21-23]. Above 25g the hardness of the sample starts decreasing up to 35g. The cracks start to occur after the load 35g. This may be due to the release of internal stress generated locally by indentation. The increasing trend of microhardness with the load up to 25g is well understood from Mayer law and onitisch condition. According to Mayer law, the relationship between the load (P) and the size (d) of the indentation is given as

$$P = k\ d^n \qquad (3)$$

where, n is called mayer index or work hardening index. Hence the slope of the plot of log P versus log d will give the work hardening index. The slope of the plot for LMN (Figure 9) is found to be 4.8. According to onitisch if n is greater than 2, the microhardness will increase with the increase of load. Hence, the material shows increasing trend for the hardness of the material up to a particular load 25g. Since LMN is having moderately higher value of hardness number, the material is found to be suitable for device fabrications until the internal stress exceeds the limit 0.35 Nm^{-2}.

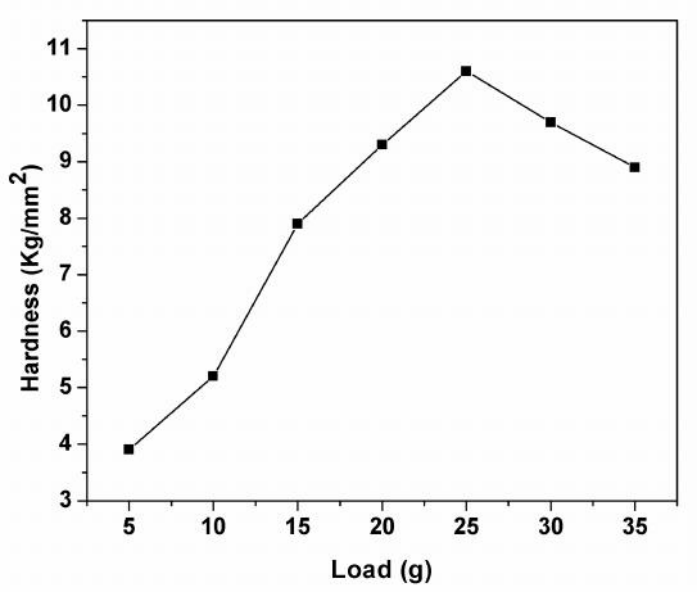

Fig. 8 Vickers microhardness of LMN crystal

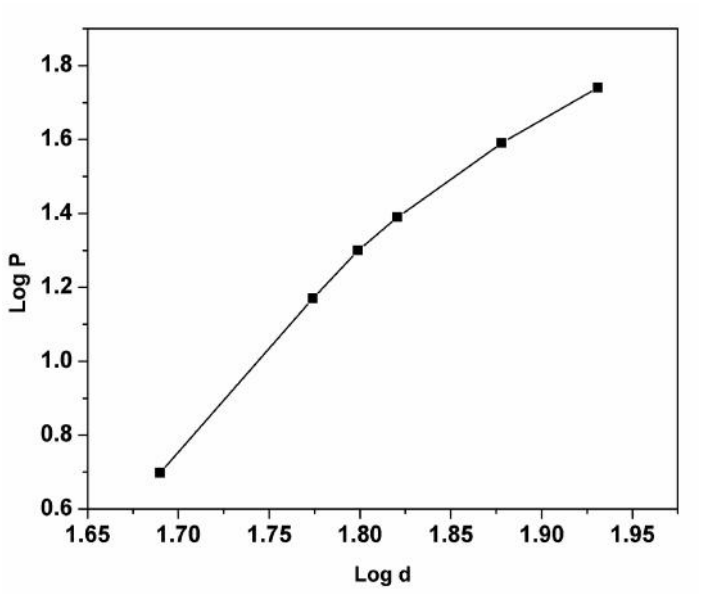

Fig. 9 Plot of log P vs log d

3.6 Second harmonic generation

Second harmonic generation of the grown crystal was confirmed using Kurtz and Perry powder technique [24]. A high intense beam of laser wavelength 1064 nm was allowed to illuminate the sample with a pulse width of 8 ns. The emission of green radiation 532 nm from the sample confirms that the material exhibits nonlinear optical property. The power of incident laser beam was measured as 0.68J. The output radiation from the crystal was allowed to fall on a photomultiplier tube which converts the light signal into electrical signal. The output power was measured as 2.86mJ. The measurements were made for some other amino acid derivatives too. LMN crystal is found to possess SHG efficiency more than that of L-alanine (2.24mJ), L-arginine bromide (2.04mJ), L-phenylalaninium maleate (1.83mJ) and L-phenylalaninium nitrate (1.76mJ). Moreover, the crystal has the advantage of combined thermal and mechanical robustness required for nonlinear optical device fabrications.

4. Conclusions

L-methioninium nitrate single crystal was successfully grown by slow evaporation technique at room temperature. Single crystal XRD study reveals that the LMN crystal belongs to monoclinic structure and non-centrosymmetirc space group $P2_1$.The functional groups of LMN crystal were identified by Fourier transform infrared spectroscopy. Molecular structure of the grown crystal was confirmed by ^{1}H NMR and ^{13}C NMR studies. The optical absorption spectral analysis reveals that the crystal is transparent in the entire UV-VIS-NIR region with the lower cut-off wavelength as 325 nm. From the thermal studies, the thermal stability was analysed. Mechanical behaviour has been studied by Vickers microharness test. Kurtz and Perry powder technique confirms that LMN is one of the promising nonlinear optical material with appreciable SHG efficiency.

Acknowledgements

One of the authors P. Vasudevan wishes to thank Sri M. Srinivasan, Chairman, and Sri K. Ramadoss, Managing Trustee of the Srinivasa Educational Trust for their support.

References

1. Fracier C.C. and Cockerham M.P., J. Opt. Soc. Am. *B*, 1987, 4, 1899-1903.
2. Prasad P., and Williams DJ; Introduction to Nonlinear Effects in molecules and Polymers, Wiley, New York, 1991.
3. Chemla D.S. and Zyss J., Nonlinear Optical Properties of Organic Molecules and Crystals, Academic Press, New York, 1987.
4. Pal T. Kar T. Bocelli G. and Rigi L., Cryst. Growth Des. 2003, 3, 13-16.
5. Rameshbabu R. Vijayan N. Gopalakrishnan R. and Ramasamy P., Cryst. Res. Technol. 2006, 41, 405-410.
6. Lydia Caroline M. Sankar R. Indirani R.M. and Vasudevan S., Mater. Chem. Phys. 2009,114, 490-494.
7. Srinivasan N. Sridhar B. and Rajaram R.K., Acta Cryst. 2001, E57, 0746.
8. Sridhar B. Srinivasan N. Dalhus B. Rajaram R.K., Acta Cryst. 2002, E58, 0779-0781.
9. Alagar M. Krishnakumar R.V. Mostad A. and Natarajan S., Acta Cryst. 2005, E 61, 01165-01167.
10. Alagar M. Subha Nandhini M.S. Krishnakumar R.V. Mostad A. and Natarajan S., Acta Cryst. 2001, E57, 0396.
11. Rajagopal K. Krishnakumar R.V. Mostad A. and Natarajan S., Acta Cryst. 2003, E 59, 031.
12. Natarajan S. Martin Britto S.A. and Ramachandran E., Cryst. Growth Des. 2006, 6, 137-140.
13. Lydia Caroline M. Prakash M. Geetha D. and Vasudevan S., Spectrochim. Acta, Part A 2011,79, 1936-1940.
14. Adhikari S. and Kar T., J. Cryst. Growth 2012, 356, 4-9.
15. Prakash M. Geetha D. and Lydia Caroline M., Spectrochim. Acta, Part A 2011, 81, 48-52.
16. Pandiarajan S, Umadevi M, Briget mary M, Rajaram RM, and Ramakrishnan V; J. Raman. Spectrosc. 2004, 35, 907-913.

17. Pandiarajan S. Sridhar B. and Rajaram R.M., Acta Crystallogr. Sect. E, 2002, 58, 882-884.
18. Caroline L. and Vasudevan S., Mater. Lett. 2009, 63, 41-44.
19. Mahalakshmi R. Jesuraja S.X. and Das J., Cryst. Res. Technol. 2006, 41,780-783.
20. Mott W., Micro Indentation Hardness Testing, Butterworths, London, 1956.
21. Zhao L. Li SB. Wen GA. Peng B. and Huang W., Mater. Chem. Phy. 2006, 100, 460-463.
22. Boomadevi S. Mittal H.P. and Dhansekararan R. J., Cryst. Growth 2004, 261, 55-62.
23. Karan S. and Gupta S.P.S., Mater. Sci. Eng., A 2005, 398, 198-203.
24. Kurtz S.K. Perry T.T., J. Appl. Phys. 1968, 39, 3798-3813.

*****